

# Microstructure of RDX investigated by means of Powder X-ray Diffraction

Michael Herrmann

Fraunhofer Institut für Chemische Technologie  
Joseph-von-Fraunhofer-Straße 7, 76327 Pfinztal  
michal.herrmann@ict.fraunhofer.de

**Keywords:** Reduced Sensitivity, Microstructure, RDX, X-ray Diffraction

## Abstract

Incorporation of improved particle qualities proved to reduce the sensitivity of plastic bonded explosives. Investigations were started using Powder X-ray Diffraction for characterizing the microstructure of the energetic nitramine RDX, including reduced sensitivity and conventional samples, and fine and coarse grades. Problems arisen from poor orientation statistics of coarse powders have been solved using advanced measuring techniques.

The investigations revealed that sensitivity of RDX correlates with crystallite size, where insensitive particles consist of larger and fewer crystallites than the conventional product.

## Introduction

The microstructure of energetic particles is in the scope of actual research. The interest stems from investigations showing that a careful processing of crystalline energetic ingredients improves the shock sensitivity of plastic bonded explosives. The mechanisms behind the sensitivity reduction are far from being clear. Particle size, shape, surface morphology, voids, inclusions, impurities, dislocations and twins are discussed to influence the mechanical sensitivity. Besides, broadly feasible methods for distinguishing conventional from reduced sensitivity (RS- or I-) products at a crystalline level are required for quality assessment.

## XRD, State of the Art

The use of diffraction line analysis for the investigation of the microstructure is nearly as old as the powder diffractometry itself. In 1918 Scherrer reported that the widths of diffraction lines are inverse to the sizes of crystallites, and 1925 Van Arkel found that lines are broadened by micro strain. Evaluation techniques described by Warren and Averbach [1] and Williamson and Hall [2] are

state of the art. The latter consists essentially in plotting reciprocal diffraction line widths  $\beta^* = \beta/\lambda \cos\theta$  versus reciprocal lattice distances  $d^* = 2/\lambda \sin\theta$ , where  $\beta$ ,  $d$ ,  $2\theta$  and  $\lambda$  are the diffraction line width, lattice distance, diffraction angle and wavelength of the radiation. If strain broadening is negligible  $\beta^*$ -values lie on a horizontal line with an intercept at the inverse of the mean linear crystallite size  $t$ . If size broadening is negligible the values lie on a straight line through the origin with the integral breadth  $\xi$  of the strain contribution as slope; provided that micro strain is isotropic. The composite peak broadening produced by simultaneous small particle size and strain depends on the broadening functions of both effects. The method solves the problem of the separation of size and strain broadening revealing the root mean square strain  $\varepsilon_{\text{rms}} = \langle \varepsilon^2 \rangle^{1/2}$  [3], which may be estimated in terms of apparent strain  $\eta_\beta = 2\beta^*_D/d^* \approx 5\langle \varepsilon^2 \rangle^{1/2}$  [4].

Contrary to powder measurements, where intensity is monitored in dependence of the diffraction angle  $2\theta$ , single crystals could be measured by means of so-called rocking curves. Within this technique radiation source and detector are positioned within a reflection condition and a crystal is tilted through its reflective orientation [5]. The resulting peak widths in terms of the sample angle  $\omega$  may also be used for characterizing crystal quality [5, 6].

### Approaches to Explosives

The investigation of explosives by means of powder X-ray diffraction XRD has already proved to be a powerful tool for characterizing polymorphism, solid state reactions, thermal expansion or phase interaction [7]. Consequentially, approaches were made to characterize the microstructure of energetic particles, based on diffraction line broadening. Investigations were started on the cyclic nitramines RDX ( $\text{C}_3\text{H}_6\text{N}_6\text{O}_6$ ) and HMX ( $\text{C}_4\text{H}_8\text{N}_8\text{O}_8$ ), as these materials are in the scope of actual research on sensitivity reduction and, moreover, provide different defect mechanisms – dislocation slip in RDX and deformation twinning in HMX. Overcoming problems of the relatively lowly absorbing nitramine, characteristic line broadening was found distinguishing HMX from RDX, and results have been discussed in terms of dislocations and twins [8].

Two advanced techniques are now being used for investigating reduced sensitivity and conventional RDX samples, taking different orientation characteristics of fine and coarse grades (C1 and C5) into account [9].

### Investigations of Fine Particles at the Synchrotron

Fine grades of conventional, reduced sensitivity and insensitive RDX with medium particle sizes of 17.6, 9.7 and 10.5  $\mu\text{m}$ , respectively, were investigated at the diff-beamline of Angström-Quelle Karlsruhe GmbH ANKA using monochrome synchrotron radiation with 1.29978 Å wavelength and a flat rotating samples holder mounted on a Bragg-Brentano diffractometer equipped with Ge-analysator crystal. Samples were measured within selected  $2\theta$ -ranges and 0.0025 ° $2\theta$  step size. With the program TOPAS from Bruker AXS peaks were indexed, and »single peaks« (with minimum or without overlap) were identified.

The single peaks were fitted using the split-Pearson VII analytical function yielding Full Widths at Half Maximum (FWHM), which were reduced by geometric peak widths determined with Lanthanum hexaboride. The data were evaluated according to Williamson and Hall [3] by plotting reciprocal peak widths versus reciprocal lattice distances, and the root mean square strains were estimated from slopes of regression lines.

Fig. 1 shows Williamson-Hall plots of the fine RDX samples, and linear regression lines  $\beta^* = a d^* + b$  fitted to selected regions of the curves. Results of the fits are summarized in Tab. 1.

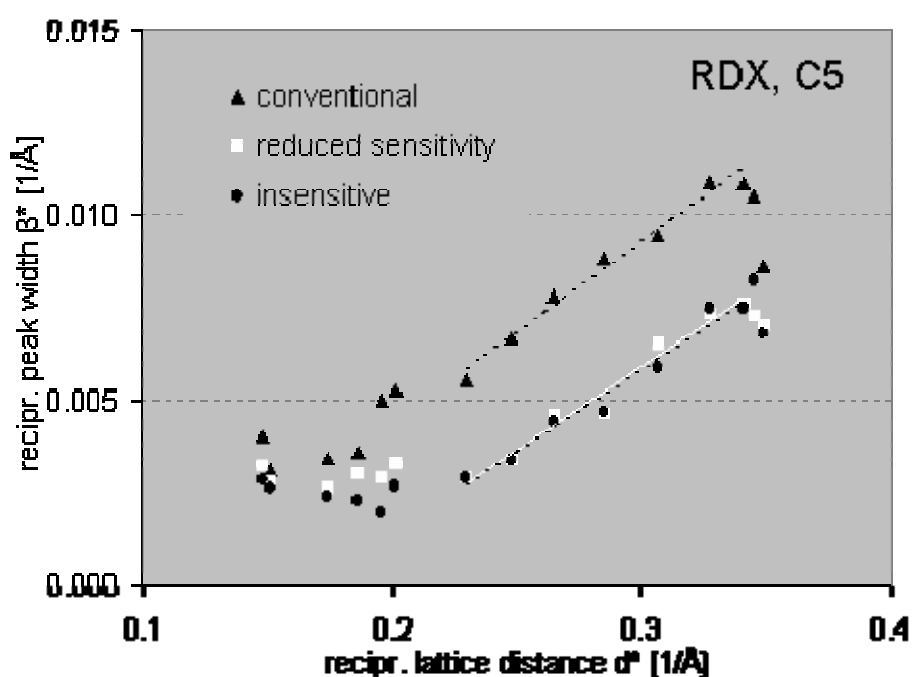


Fig. 1: Williamson-Hall plot of RDX, RS-RDX and I-RDX. Varying level of curves identify differences of crystallite size.

Tab. 1: Coefficients of regression lines  $\beta^* = a d^* + b$  and estimated root mean square strain  $\epsilon_{rms}$ .

Sample	a	b [1/Å]	$\epsilon_{rms}$
RDX	0,049	-0,0055	0,02
RS-RDX	0,045	-0,0074	0,018
I-RDX	0,044	-0,0076	0,018

The RDX curves run linear between 0.23 and 0.34 1/Å, bending up at low  $d^*$ -values and down at high values. Some regression lines would intercept the y-axes at negative values ( $b$ ) which physically doesn't make sense. The effect

is attributed to estimating geometrical peak widths as no lowly absorbing size/strain reference for the low  $2\theta$ -region has been available. The slopes are in a reasonable range, but may also be influenced by this effect. However, the values are evaluated relatively, meaning that e.g. lower intercept values represent larger crystallite sizes and vice versa.

The plots revealed approximately same curves for RS- and I-RDX but clearly distinguished from the curve of the conventional sample. The estimated root mean square strain of the RDX is with 0.02 slightly higher than the values of RS-RDX and I-RDX with 0.018. More pronounced are the differences of the levels and intercepts of the curves, pointing to significantly smaller crystallites in the conventional RDX.

### Rocking Curves of Coarse Particles

The disadvantage of poor orientation statistics of coarse samples for standard diffraction techniques may be inverted into an advantage, when reflections from isolated domains could be evaluated separately. While measuring a rocking curve, domains are tilted in and out of their reflection conditions, randomly. For a coarse powder and not too much particle in the sample, reflections may be separated and evaluated statistically.

Coarse grades of conventional, RS- and I-RDX with particle sizes of 195, 205 and 225  $\mu\text{m}$ , respectively, were investigated on a D5000 Bragg-Brentano diffractometer from Bruker AXS equipped with copper tube, vertical soller slits, Ni- $k_{\beta}$ -filter and scintillation counter. Measurements were performed on reflections (111), (200), (002), (220) and (131). For each reflection the sample was tilted from  $\omega = \theta - 5^\circ$  to  $\theta + 5^\circ$  with 0.005  $^\circ$  step width and 6 s step time;  $\theta$  represents the symmetric position.

Pearson VII analytical functions were fitted to the diffraction profiles yielding intensities and Full Widths at Half Maximum (FWHM) of each dissolvable peak. The obtained data were evaluated by plotting the normalized additive number of peaks versus peak widths and by determining median peak widths  $X_{50}$  and slopes of the curves around this value estimated by  $X_{25}/X_{75}$ .

Fig. 2 shows rocking curves of reflections (111), (200) and (002) measured with RS-RDX. The normalized additive number of peaks is plotted versus peak widths FWHM in Fig. 3 for reflection (111). The median peak widths  $X_{50}$  and quotients  $X_{25}/X_{75}$  are summarized in Tab. 2, where values in brackets give standard deviations determined from five freshly prepared measurements of RS-RDX. The median peak widths of the coarse samples plotted separately for each measured reflection are shown in Fig. 4. Lowest median peak widths are found for I-RDX between 0.03 and 0.038  $^\circ\omega$  followed by values of RS-RDX between 0.038 and 0.054  $^\circ\omega$  and RDX between 0.052 and 0.077  $^\circ\omega$ .

Considering standard deviations about 0.006  $^\circ\omega$ , the differences prove to be significant. The  $X_{25}/X_{75}$  values of I-RDX around 0.52 represent steeper curves than those of RS-RDX and RDX around 0.4 and 0.45; meaning that the strain or size distribution is narrower in I-RDX than in RS-RDX and RDX. The plot of the median peak widths in Fig. 4 shows that anisotropic peak broadening is

most pronounced for RDX, whereas values of I-RDX are approximately independent on peak indexing.

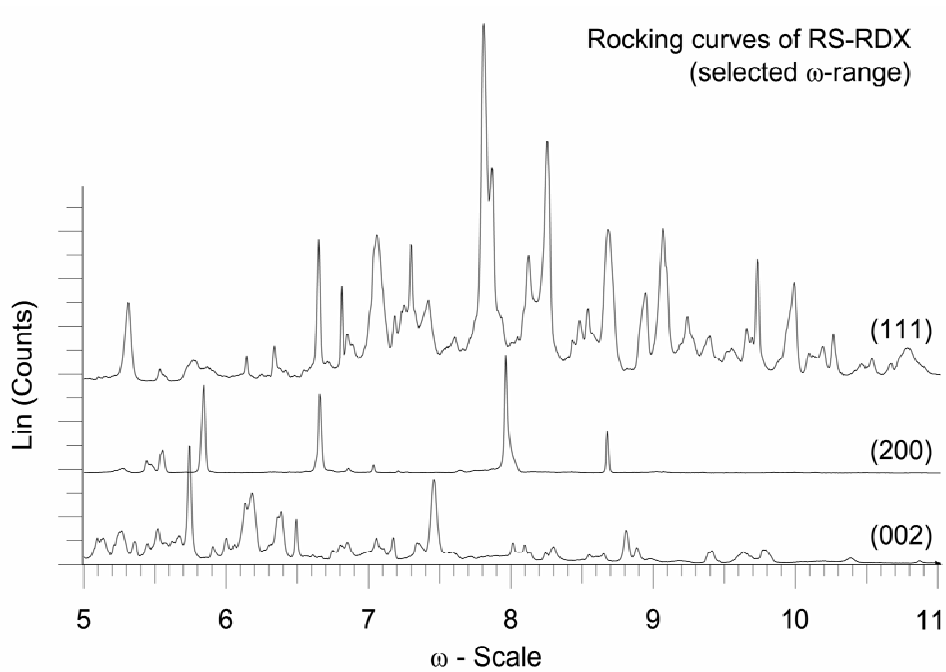


Fig. 2: Rocking curves of reflections (111), (200) and (002) measured with RS-RDX.

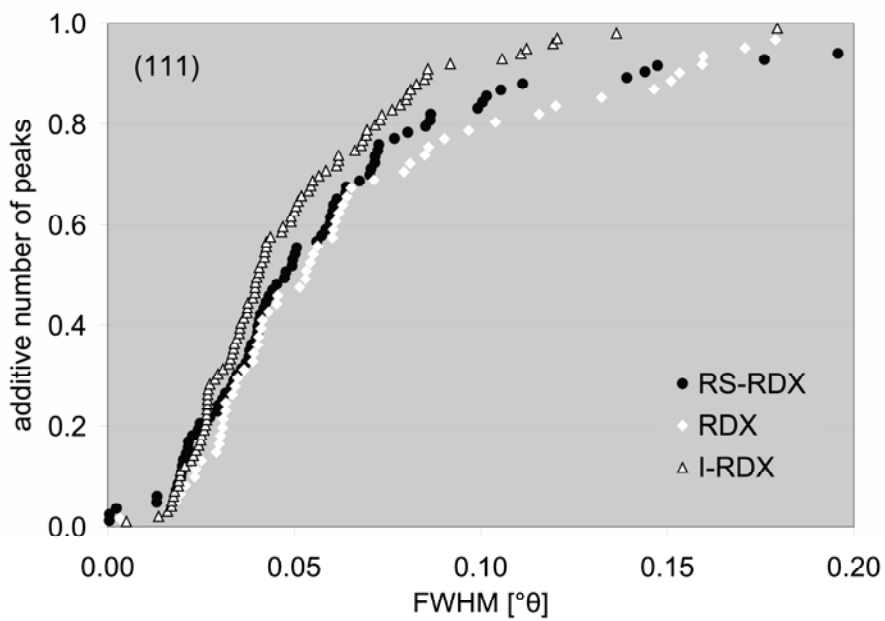


Fig. 3: Normalized additive number of peaks plotted versus peak width of reflection (111)

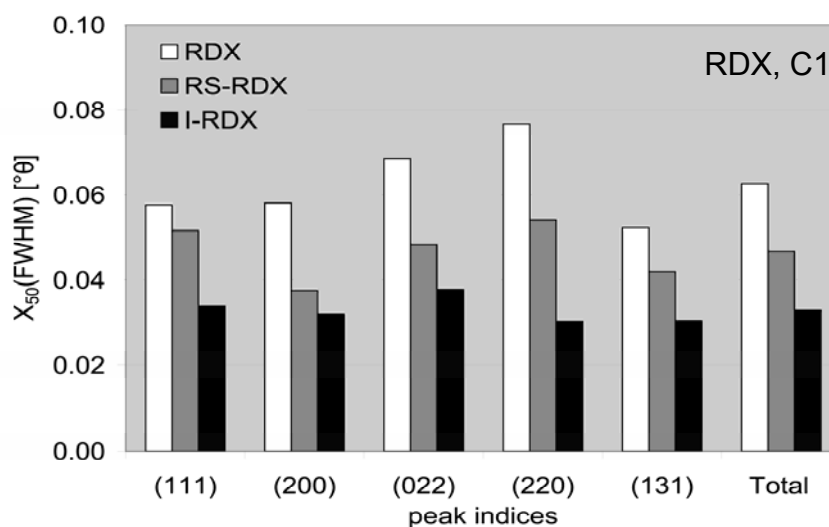


Fig. 4: Median peak widths  $X_{50}$  of rocking curves plotted versus peak indices. Low values of I-RDX and RS-RDX identify higher crystal qualities of these samples compared to the conventional RDX.

Tab. 2: Median peak widths  $X_{50}$  and quotient  $X_{25}/X_{75}$  of coarse RDX samples obtained from rocking curves (standard deviations in terms of last digit of related value are given brackets).

Peak	RS-RDX		I-RDX		RDX	
	$X_{50}$ [°ω]	$X_{25}/X_{75}$	$X_{50}$ [°ω]	$X_{25}/X_{75}$	$X_{50}$ [°ω]	$X_{25}/X_{75}$
(111)	0.052(3)	0.43(4)	0.034	0.47	0.058	0.42
(200)	0.038(6)	0.34(8)	0.032	0.51	0.058	0.53
(022)	0.048(7)	0.46(5)	0.038	0.52	0.069	0.48
(220)	0.054(7)	0.35(4)	0.030	0.54	0.077	0.35
(131)	0.042(7)	0.44(7)	0.030	0.55	0.052	0.45
mean	0.047	0.40	0.033	0.52	0.063	0.45

## Conclusions

The investigations show that qualities of explosive powders can be distinguished on the bases of their microstructure using powder X-ray diffraction. Problems arisen from low absorbance or poor orientation statistics of coarse powders have been solved by advanced techniques using synchrotron radiation or rocking curves.

The I-RDX and RS-RDX show significantly narrower diffraction peaks than the RDX; fine and coarse grades. The broadening was attributed to smaller crystallites in the conventional RDX compared to the insensitive variants I-RDX and RS-RDX. On the other hand the particle size of the conventional product is larger than those of I-RDX and RS-RDX. This leads to the hypothesis that RDX particles consisting of few large crystals or even a single crystal are less

sensitive than those of many small crystals. The crystal or grain boundaries and dislocations within these boundaries may ease undergoing a reaction.

### Acknowledgements

ANKA is gratefully acknowledged for beam time, and particularly Dr. Stephen Doyle for his kind help and fruitful discussions during the measurements at the synchrotron.

Harald Fietzek and Bastian Ludwig from Fraunhofer ICT are acknowledged for performing the laboratory X-ray diffraction experiments.

Parts of this material are based upon work supported by the European Office of Aerospace Research and Development, London, under Contract No. FA8655-05-1-3029.

### References

- [1] B. E. Warren, B. L. Averbach, The effect of Cold-Worked Distortion on X-Ray Patterns. *J. Appl. Phys.* **1950**, V21, 595-599.
- [2] G. K. Williamson, W. H. Hall, X-ray Line Broadening from fcc Aluminum and Wolfram. *Acta Metall.* **1953**, V1, 22-31.
- [3] T. Ungár, Warren-Averbach Applications, in *Industrial Applications of X-Ray Diffraction* (Eds.: F. H. Chung, D. K. Smith), Marcel Dekker, Inc., New York, Basel, **2000**, 847-867.
- [4] J. I. Langford, Line Profiles and Sample Microstructure, in *Industrial Applications of X-Ray Diffraction* (Eds.: F. H. Chung, D. K. Smith), Marcel Dekker, Inc., New York, Basel, **2000**, 751-775.
- [5] J. R. Schneider, Interpretation of Rocking Curves Measured by  $\gamma$ -ray Diffraction. *J. Appl. Cryst.* **1974**, 7, 547-554.
- [6] L. Spieß, R. Schwarzer, H. Behnken, G. Teichert, *Moderne Röntgenbeugung*, BG Teubner Verlag, Wiesbaden, **2005**, 282-284.
- [7] L. Borne, M. Herrmann, C. B. Skidmore, Microstructure and Morphology, in *Energetic Materials – Particle Processing and Characterization* (Ed. U. Teipel), WILEY-VCH, Weinheim, **2005**, 333-366.
- [8] M. Herrmann, H. Fietzek, Investigation of the Microstructure of Energetic Crystals by means of X-ray Powder Diffraction. *Powder Diffraction* **2005**, 20 (2), 105-108.
- [9] M. Herrmann, Microstructure of Energetic Particles Investigated by X-ray Powder Diffraction, Submitted: *J. Particle and Particle System Characterization*, February **2006**